Roles of strike-slip faults during continental deformation: examples from the active Arabia-Eurasia collision

Mark B. Allen

Department of Earth Sciences, University of Durham, Durham, DH1 3LE, UK

Abstract: This paper concerns the kinematics of active strike-slip faults in the Arabia-Eurasia collision zone, and how they accommodate plate convergence. Several roles are discernible. *1) Collision zone boundaries* – the left-lateral Dead Sea Fault System and right-lateral faults in eastern Iran form the western and eastern boundaries of the collision zone. *2) Tectonic escape structures* – the North and East Anatolian faults transport intervening crust westwards, out of the path of the Arabia. *3) Strain partitioning* – right-lateral slip on the Zagros Main Recent Fault and NW-SE striking thrusts to its SW produce north-south convergence, parallel to the plate vector. Left-lateral slip along the Alborz range and thrusts across it produce oblique left-lateral shortening. *4) Shortening arrays* – arrays of strike-slip faults (e.g. Kopeh Dagh and eastern Iran) rotate about vertical axes, producing north-south shortening without crustal thickening. *5) Transfer zones* – fold trends and earthquake slip vectors change orientation across strike-slip faults in the Zagros, suggesting that these faults allow for changes in thrust transport along strike in the orogen. These different roles emphasise the complex behaviour of continental crust, and the advantages of studying active tectonics rather than ancient examples.

Introduction

This paper reviews active strike-slip faults from the Arabia-Eurasia collision zone (Figures 1, 2 & 3), to summarise the different ways such faults help achieve plate convergence during continent-continent collision. This is an important issue for two reasons. The first is that it is part of the more general problem of how faults in the upper crust collectively produce the velocity fields required by plate motions. The second is that strike-slip faults are common features in the geological record of the continents, but it is not always easy to determine why such faulting took place. Active tectonics provides data and constraints not available in ancient settings, principally through studies of decadal to millennial slip vectors (via GPS and seismicity studies) and through use of the landscape to deduce deformation patterns. The approach is to use case studies from different regions to make general conclusions about the way the strike-slip faults in the upper crust behave during continental deformation. It is not intended to be a systematic account of every active strike-slip fault in SW Asia, nor does it dwell on the many other aspects of the collision. Other papers (e.g. Mann, 2007) synthesise the structures associated with continental strike-slip faults, regardless of their origins: such material is not repeated here.

Active slip rates and finite offsets are known for many of the strike-slip faults, and in some cases there are data for the timing of onset. Therefore it is possible to compare the patterns of short-term and long-term deformation in the collision zone, and by implication in continental crust in general. Strike-slip faults are easier to work with in this respect than thrusts or normal faults, where the overall shortening or extension may be poorly constrained through lack of sub-surface data.

Continental collision zones are excellent places in which to study continental deformation processes in general because of the widespread and highly variable nature of the deformation that takes place. Although collision by definition implies plate convergence, this can be accommodated in a tremendous variety of ways by combinations of compressional, strike-slip and even extensional structures (Dewey et al., 1986). Faulting is the main way in which strain is accomplished within the brittle upper crust, therefore the kinematics of fault zones are revealing about overall strain. However, there are few active continental collision zones in the world, compared with active subduction zone boundaries for example. One is the Arabia-Eurasia collision, part way along the network of Cenozoic orogenic belts between the Pyrenees and SE Asia known collectively as the Alpine-Himalayan system. Following a geological overview of the collision, later sections focus on individual faults and groups of faults, to show how their kinematics fit in to the overall plate convergence. Figure 3 is a summary map of the main active strike-slip faults in the Arabia-Eurasia collision, but also highlights the generic roles outlined in this paper, namely: collision zone boundaries (Dead Sea Fault system, eastern Iranian faults); tectonic escape structures (North and East Anatolian faults); strain partitioning elements (Main Recent Fault of the Zagros; Mosha Fault in the Alborz); shortening arrays (Kopeh Dagh); transfer and tear faults (Sangavar Fault).

Geological background

Collision between Arabia and Eurasia initially took place along the Bitlis-Zagros suture, which curves through SE Turkey before running NW-SE through southern Iran (Figure 1). The plate boundaries were a passive continental margin on the

northern side of the Arabian plate and an active continental margin along southern Eurasia (Şengör et al., 1988; Beydoun et al., 1992).

The plate scale present-day convergence between Arabia and Eurasia is well-understood: GPS studies show that roughly 18±2 mm/yr north-south convergence takes place between the stable interiors of Arabia and Eurasia at longitude 48^{o}E (Figure 1; McClusky et al., 2000). Convergence velocities increase and azimuths swing anti-clockwise west to east along the collision zone, with a rotation pole in the northeast Africa/eastern Mediterranean region (McClusky et al., 2003) and velocities ~10 mm/yr higher in eastern Iran than the western side of the collision. GPS and seismicity studies together show that deformation is concentrated between the Persian Gulf and the north side of the Greater Caucasus and Kopeh Dagh ranges – there is a good correlation between the limits of seismicity and topographic fronts (Figure 2). But deformation is not distributed evenly within these northern and southern limits. Seismogenic thrusting, and hence plate convergence achieved by crustal shortening *and* thickening, is presently concentrated in areas below the 1 km topographic contour (Talebian and Jackson, 2004). This is mainly within the lower parts of the Zagros and Alborz/Caucasus regions at the southern and northern sides of the collision respectively (Figure 3). The intervening region has lower relief, elevations commonly over 1.5 km and is known as the Turkish-Iranian plateau. GPS data from within the collision zone reveal that little active internal shortening takes place within this plateau (~2 mm/yr or less; Vernant et al., 2004a), and large areas are aseismic. It is not totally quiescent: Late Cenozoic volcanics occur in discrete fields across it (Pearce et al., 1990; Kheirkhah et al., 2009), and strike-slip faults are locally associated with historical earthquakes, indicating at least some tectonic activity (Copley and Jackson,

2006). Another area of low internal deformation at present is the South Caspian Basin, north of the Alborz (Figure 3). Para-oceanic basement to this basin is in the early stages of subducting under the northern and possibly western basin margins (Mangino and Priestley, 1998; Jackson et al., 2002). This basement is detached from folds within the thick sedimentary cover: these folds are not typically associated with major seismicity, indicating that the basement behaves as a rigid block, presumably because of unusually strong basement.

The western margin of the collision zone is sharply defined along the Dead Sea Fault System, which allows the largely stable interior of Arabia to move northwards with respect to the eastern Mediterranean. This basement to the latter area is not well known as it is buried beneath a thick sedimentary cover, including salt. It is probably underlain by highly thinned continental or even oceanic crust (de Voogd et al., 1992). West of a triple junction at the northern end of the Dead Sea Fault System, subduction of eastern Mediterranean basement takes places along the Cypriot and Hellenic arcs. Collision has not yet taken place in these regions, and north of the Hellenic arc the Aegean crust is rapidly extending. This extensional province merges eastwards in onshore Turkey, in to the crust of Anatolia. Here there is little active internal deformation, but wholesale westwards transport between the North and East Anatolian faults (McKenzie, 1972). The eastern side of the collision roughly coincides with the political boundary of Iran and Afghanistan; the latter is part of stable Eurasia, in the context of the active deformation field. There is active subduction of Indian plate oceanic lithosphere under the Makran (Regard et al., 2005).

Less is known about the earlier evolution of the collision zone. Even the onset of collision is debated, with recent estimates ranging from Late Eocene (~35 Ma) to mid-late Miocene (12-10 Ma) (McQuarrie et al., 2003; Vincent et al., 2005; Guest et al., 2006a; Verdel et al., 2007). Allen & Armstrong (2008) proposed that there was evidence from many localities both sides of the original suture for Late Eocene (~35 Ma) deformation, uplift or changing sedimentation patterns, and that this was the true time of initial collision. This debate on the collision timing highlights how difficult it can be to interpret geological data from ancient settings. It arises in part because we can never have an overview for past times across the entire orogen, in the way that remote sensing, seismicity and GPS all provide for the active tectonics. Therefore data from one region for initial rock uplift, say, can get treated as though it is representative of the entire collision zone. This is misguided, given how the present day tectonics show the wide variety of deformation, and quiescence, that takes place at any one time.

As a general point, there is no systematic difference in the depths of the strike-slip and thrust earthquakes in the various regions of the collision zone, such as the Alborz and Zagros ranges (Figure 3). They are typically up to ~15-20 km, i.e. within the crystalline basement of the crust (Jackson et al., 2002; Talebian & Jackson, 2004). This indicates that the strike-slip deformation described in this paper is “thick-skinned” in structural geology terms.

Collision zone boundaries

Reduced to its simplest, the Arabia-Eurasia collision represents ~north-south convergence between a promontory (Arabia) and a much broader continental mass

(Eurasia). Figure 4 is a cartoon that highlights the main elements of the collision, and illustrates the role of strike-slip faults and the boundaries of deformation. The real locations of these structures are shown on Figure 3. The pre-collision position of the Arabian and Eurasian plate margins is not precisely known, but the north-south convergence vector requires hundreds of kilometres of northwards motion of the stable interior of Arabia with respect to stable Eurasia, over tens of millions of years (McQuarrie et al., 2003; Allen & Armstrong, 2008). Therefore it is unsurprising that the northern and southern limits to deformation are marked by thrusting (Figure 2) – allowing for plate convergence via crustal thickening, whereas the western and eastern limits are strike-slip fault zones – allowing the Arabian plate to move past adjacent crust. A crucial difference between the strike-slip faults on the western and eastern margins of the collision is that the former, the Dead Sea Fault System, decouples Arabia from the eastern Mediterranean, but both regions were part of the combined African-Arabian plate before collision. In the case of the east Iranian faults, the great majority of the region involved was part of Eurasia before the initial collision.

Deformation is sharply focused along the ~1000 km long, left-lateral Dead Sea Fault System (Garfunkel, 1981; Figure 3), except for local splays at releasing and restraining bends such as the Dead Sea pull-apart basin (Manspeizer, 1985) and the Mount Lebanon range. The southern end of the fault links in to the active extension within the Red Sea: debate continues as to the interaction of extension in this region and initial collision on the northern side of the Arabian plate (Jolivet and Faccenna, 2000; McQuarrie et al., 2003). The northern end links in to the folds and thrust belts in southeastern Anatolia and the Zagros. Total offset across the fault is ~105 km south

of the Dead Sea (Quennell, 1958), and this is fully observed in an offset dyke swarm dated at 22-18 Ma (Eyal et al., 1981). Active and late Quaternary slip rate estimates are variable, at 2-8 mm/yr (e.g. Klinger et al., 2000), although more recent studies are producing values of ~5 mm/yr (Ferry et al., 2007; Gomez et al., 2007). This velocity would need ~20 million years to achieve the full offset, consistent with the age of the offset dykes, but inconsistent with the fault having operated at this slip rate since the proposed Late Eocene start of collision.

North-south right-lateral faulting in eastern Iran form the eastern boundary to the collsion zone (Figures 1-3). Oceanic subduction takes place under the Makran region, such that right-lateral faults in the extreme southeast of Iran juxtapose the easternmost Zagros (originating on the Arabian passive margin) with the accretionary prism to the east (Regard et al., 2005; Bayer et al., 2006). Further north, right-lateral faults to the east (Neh and Zahedan) and west (Nayband and Gowk) of the inert Dasht-e-Lut have a total offset estimated by Walker and Jackson (2004) as ~80 km. A difference between the eastern and western margins to the collision zone is that in the west there is only one, whereas in eastern Iran there are at least two active, parallel fault systems, and possibly several more. There is little doubt that the Nayband and Gowk faults and the Neh and Zahedan faults take up most of the slip between Iran and Afghanistan (Walker and Jackson, 2004; Walker et al., 2009), but the Deh Shir, Anar and Kuh Bahnan faults are also active (Meyer, 2006; Meyer and LeDortz, 2007), plausibly slip at 1-2 mm/yr in the Holocene, and so may contribute part of the overall shear. A more fundamental problem is why deformation is so focused at the western collision margin, and distributed in the east. The reason may be the distinct contrast in crustal type at the western side, where the Arabian crust was juxtaposed with para-oceanic

197 basement to the eastern Mediterranean long before initial collision, when both regions
198 formed part of the passive margin at the northern side of the African-Arabian plate. In
199 eastern Iran and Afghanistan there is a mosaic of similar Gondwana-derived basement
200 blocks (Şengör et al., 1988). Those blocks east of the Arabian indentor are not being
201 deformed by the Arabia-Eurasia collision, but there is no sharp contrast within this
202 crust as there is in the west.
203
204 The GPS derived right-lateral shear between eastern Iran and Afghanistan is ~16
205 mm/yr (Vernant et al., 2004a). This only requires 5 million years to achieve the total
206 observed offset along the Neh/Zahedan and Nayband/Gowk faults. Given that all
207 estimates of the initial collision put it much earlier than 5 Ma, something else
208 accomplished right-lateral shear at the eastern side of the collision. The obvious
209 explanation is that the region must contain faults that are now inactive, or only weakly
210 active. The Deh Shir, Anar and Kuh-e Bahnan faults may have contributed relatively
211 more to the boundary shear in the past, regardless of their precise present
212 contribution. There may be further structures within the deserts of eastern Iran as yet
213 unquantified or unrecognised.
214
215 **Tectonic escape structures**
216 The Arabia-Eurasia collision zone contains the first recognised example of so-called
217 escape tectonics, in the case of Anatolian crust between the North and east Anatolian
218 faults (McKenzie, 1972). These are active right- and left-lateral faults respectively,
219 and act to transport intervening crust westwards, largely without internal deformation
220 (Figure 1). Figure 4 reduces the kinematics to their simplest. The left-lateral East
221 Anatolian Fault is the boundary between Arabia and Anatolia (Figure 3), and runs for

~400 km southwest of its intersection with the North Anatolian Fault at Karliova, at approximately 39.5^{o} N 41^{o} E. There are several strands to the fault zone, with localized pull-apart basins and push-up zones (Lyberis et al., 1992; Westaway, 1994). The GPS-derived slip rate is 9±1 mm yr-1 (McClusky et al., 2000) only needs to operate for ~3 million years to achieve the geological offset of 27-33 km (Westaway and Arger, 1996; Westaway et al., 2006), constrained by offset geological markers. This is in good agreement with the age of initial offset as late Pliocene (~3 Ma) or younger (Şaroğlu et al., 1992; Westaway and Arger, 2001), based on the offset of volcanics of this age.

The right-lateral North Anatolian Fault (NAF) achieves the slip between Eurasian and Anatolian crust for >1200 km (Figures 1 and 2), at a GPS-derived slip rate of 24±1 mm yr-1 (McClusky et al., 2000). The western end of the fault splits where it enters the north Aegean and passes in to the extensional deformation in that region. Roughly 80-85 km is emerging as a consensus figure for the total offset of most of the length of the fault zone, based on combinations of geological and drainage offsets (Armijo et al., 1999; Westaway, 1994; Seymen, 1975). Distributed strike-slip and/or extension took place in the mid or late Miocene, before the establishment of the present fault trace in some regions (e.g. Barka and Hancock, 1984; Tüysüz et al., 1998; Coskun, 2000; Şengör et al., 2005). There is no consensus on a precise age for the start of motion on the NAF, despite several estimates of ~5 Ma (see Bozkurt, 2001). The GPS-derived slip rate (24±1 mm/yr) achieves the total offset of 80-85 km in only ~3.5 million years, less than most geological estimates for the fault age. It seems that: i) the slip-rate is higher now than in the past (but this is uncertain), and ii) the fault has not been active since the start of collision (this is more definite).

Like the Dead Sea Fault System, the narrowness of both the NAF and EAF and the sharp velocity contrasts across them resemble plate boundaries, as utilised as long ago as McKenzie (1972) in his vector calculations. But this is a nearly instantaneous picture, and it is striking that both faults are young with respect to the overall collision zone, and need only a few million years at their present slip rates to achieve their total offset. In the case of the EAF, other faults may have played similar kinematic roles in the past. Other (inactive?) left-lateral faults have been identified in eastern Turkey, such as the Malatya-Ovacik Fault (Westaway and Arger, 2001), with ~29 km offset between 3-5 Ma, and the Ecemiş Fault (Jaffey and Robertson, 2001), with ~60 km offset, mainly between the Late Eocene and Miocene. Activity on the Central Anatolian Fault (Kocyigit and Beyhan, 1998) is disputed (Westaway, 1999). However, as the triple junction at the eastern end of NAF and EAF should migrate west with time, it is difficult to see how any of these inactive left-lateral faults in eastern Anatolia were the precise equivalent of the modern EAF.

Elements in strain partitioning

Plate boundaries are rarely orthogonal to plate vectors (Woodcock, 1986). This fact underlies the origins of many continental strike-slip faults, not only in collision zones. Accommodation of north-south convergence by east-west trending faults would be likely in idealised, isotropic crust, but has not happened in the heterogeneous crust of both Arabia and Eurasia. The suture zone trends NW-SE for much of its length (mainly within Iran), at roughly 45^{o} to the plate convergence vector. Pre-collision structural fabrics commonly lie parallel to the suture within both plates (e.g. Sarkarinejad et al., 2008). The pattern of active faulting in the Zagros strongly

suggests pre-collision normal faults in the Arabian passive margin are now active as thrusts. Conclusive evidence for individual fault reactivation is rarely available, largely because of a thick sediment carapace over blind thrusts, but most folds and thrusts in the northwest Zagros trend NW-SE, parallel to both the suture and the trend of pre-collision sediment isopachs (Beydoun, 1992). The resultant NE-SW shortening is therefore oblique to the north-south plate convergence, and cannot achieve it on its own. The answer is the combination of this thrusting with adjacent strike-slip faulting, in an example of so-called strain partitioning (Figure 4).

Along the northeast side of the Zagros, loosely along the line of the original suture, there is a right-lateral strike-slip fault, the Main Recent Fault (MRF) (Talebian and Jackson, 2002; Figure 3). Offset along the MRF is ~50 km (Talebian and Jackson, 2002). Shortening across the widest structural unit in the Zagros, the Simple Folded Zone, is similar in magnitude (Blanc et al., 2003; McQuarrie, 2004). Combining the two estimates suggests ~70 km of north-south convergence across the Zagros, by applying Pythagoras' rule (Figure 5A). This is only valid if the strains took place at the same time. It is clear that shortening across the Zagros is active, and focused on lower elevations (<1 km) in the Simple Folded Zone. Vernant et al. (2004a) estimated 6.5±2 mm/yr north-south convergence at longitude ~51^{o}E, in their GPS survey of Iran. Likewise, both seismicity and GPS data indicate right-lateral slip along the Main Recent Fault, and the difference in slip vector azimuths between the Main Recent Fault and the Simple Folded Zone emphasise the effectiveness of partitioning. But the active slip rates do not fit a Pythagorean triangle as neatly as the total displacements, because GPS-derived slip along the MRF is only 3±2 mm/yr (Vernant et al., 2004a). This is less than the expected ≥10 mm/yr, if the onset of slip was ≤5 Ma (Talebian and

297 Jackson, 2004). A further complication is that the Simple Folded Zone deformation
298 may have begun earlier than 5 Ma, as suggested by syn-fold deposition at ~8 Ma near
299 the Zagros foreland (Homke et al., 2004).
300
301 Another example of strain partitioning in the active collision zone is from the Alborz
302 mountains of northern Iran (Jackson et al., 2002; Allen et al., 2003; Guest et al.,
303 2006b). This range lies between the Turkish-Iranian plateau to the south and the South
304 Caspian Basin to the north (Figure 3). It is actively thrusting to both the north and
305 south, and cut by range-parallel left-lateral strike-slip faults with offsets in the order
306 of several tens of kilometres (Mosha, Astaneh; Figure 6) (Allen et al., 2003; Ritz et
307 al., 2006; Hollingsworth et al., 2008). These are apparently segmented along strike,
308 and at least locally more than one parallel fault segment is active – such as the
309 Damghan Fault south of the longer Astaneh Fault. The resultant oblique motion
310 across the range allows for westward motion of the rigid South Caspian basement
311 with respect to Iran. Like the Zagros, the variation in earthquake slip vector azimuths
312 helps make the case for effective strain partitioning (Jackson et al., 2002). Thus in
313 contrast to the Zagros example, the strike-slip component of oblique shortening takes
314 place predominantly within the thrust belt (Figures 5B and 6). Vernant et al. (2004b)
315 determined the north-south shortening rate across the Alborz as 5±2 mm/yr and the
316 left-lateral shear as 4±2 mm/yr, from a GPS study. Ritz et al. (2006) identified an
317 extensional component on some of the left-lateral faults, which they suggested
318 represented a Quaternary re-organisation of the deformation.
319
320 There is evidence for older, but probably late Cenozoic, right-lateral faulting along
321 parts of the range (Axen et al., 2001; Allen et al., 2003; Guest et al., 2006b; Zanchi et

al., 2006). Thus at least part of the Alborz strike-slip system shows evidence of rapid reversal of its sense of motion, possibly within the last few million years. Given that the folding within the South Caspian cover succession is only a few million years old at most (Devlin et al., 1999), the overall westward motion of the South Caspian basement is very young (Jackson et al., 2002), the present fault configuration may be as recent as the Quaternary (Ritz et al., 2006). In contrast, Hollingsworth et al. (2008) showed that present slip rates in the eastern Alborz require ~10 million years to achieve the total offset, suggesting that the present kinematics go back further in time.

The combination of left-lateral faulting along the Alborz and right-lateral along the Zagros has attracted repeated interest over the years, promoting the idea of eastwards escape of Iranian crust out of the collision zone, in an apparent mirror image to the westwards transport of Anatolian crust (McKenzie, 1972; Axen et al., 2001; Bachmanov et al., 2004). Both seismicity data (Jackson et al., 1995) and the GPS-derived velocity field (Vernant et al., 2004a) show that this is not the case (Figure 1), and that the strike-slip faults parallel to each range help accommodate oblique convergence across them (Allen et al., 2006). It the case of the Zagros, the resultant convergence is parallel to the regional plate vector. The Alborz strike-slip relates to the South Caspian basement moving as a rigid block within the collision zone, at a high angle to the overall plate convergence vector. This case study is a warning for all interpretations of escape tectonics in ancient orogens, where seismicity data and GPS-velocity fields are not feasible and the regional plate kinematics are not known: it is possible that such settings represent the strike-slip component of strain partitioning as outlined here. It should be feasible to distinguish between real and illusory escape tectonics, given that an essential component of strain partitioning is an adjacent zone

of contemporary thrusting. In Anatolia, the neotectonic strike-slip faulting postdates previous thrusting and thickening.

Jackson (1992) noted that pure dip slip thrusting in the Greater Caucasus took place on slip vectors oriented clockwise of the overall convergence vector at this longitude. The overall convergence vector is achieved by combining this shortening in the Greater Caucasus with right-lateral strike-slip faulting to the south, within the Lesser Caucasus and the interior of the Turkish-Iranian plateau. This is most active in a WNW-ENE trending swarm of right-lateral faults including Van (Figure 3). Copley and Jackson (2006) also found that an array of NW-SE right-lateral strike-slip faults accommodate a NW-SE velocity gradient of NE directed velocity; these faults are located between the Van and Sevan faults. An aspect of this right-lateral shear within the Turkish-Iranian plateau (south of the Greater Caucasus) is that it is distributed across many faults, rather than focused on one main structure, which is the case to the west and SE in the NAF and Main Recent Fault respectively. In part this may be because of the presence of linear pre-Cenozoic sutures in the latter areas, available for reactivation. But it also relates to the way strain is partitioned across a much wider area than either the Zagros or Alborz, with the shortening component in the Greater Caucasus located north of the strike-slip faults (Jackson, 1992). The strike-slip fault system is constantly transported northwards by the shortening in the Greater Caucasus, in a way that does not happen in either the Alborz or Zagros.

Shortening arrays

Escape tectonics is one scenario where continental shortening takes place without crustal thickening. Strike-slip faults can achieve crustal shortening in another way, via

arrays of en echelon faults rotating about vertical axes as they slip (Figure 4). The situation has parallels with the behaviour of normal faults in rift zones; in the latter case the faults rotate about horizontal axes as they slip and thin and extend the crust. In the strike-slip setting the net result is shortening across the fault zone and lengthening along it. Such fault arrays have recently been recognised in several places within the Arabia-Eurasia collision zone, mainly by James Jackson and colleagues.

The Kopeh Dagh in northeastern Iran lies on the northern side of the collision, between the Turkish-Iranian plateau to the south and the undeformed crust of the Turan platform to the north (Figure 3). Its structure is dominated by arcuate but broadly NW-SE trending folds and thrusts, which deform and expose Mesozoic and Lower Tertiary strata at current exposure levels. The right-lateral and range-parallel Ashkabad Fault lies along the northeastern margin of the range, trending WNW-ESE, such that the combination of slip along this fault and shortening/thickening across the range is another example of strain partitioning in the collision zone (Lyberis and Manby, 1999). But the folds and thrusts are offset by an en echelon array of right-lateral faults that strike NNW-SSE or NW-SE (Hollingsworth et al., 2006), such as the Quchan Fault. Palaeomagnetic data are not available to quantify tectonic rotations, but the folds of Mesozoic strata can be traced across the fault zones and the rotations thereby quantified. Knowing the rotations and the present dimensions of the fault arrays allows the total north-south shortening achieved by these faults to be estimated as ~60 km (Hollingsworth et al., 2006). The geometry of such a fault array is shown schematically on Figure 7. GPS data (Vernant et al. 2004a) put the total north-south convergence across the Kopeh Dagh as ~7 mm/yr. As there are no detailed estimates

for crustal shortening via thrusting and thickening, it is difficult to compare geodetic and long-term deformation rates across the range.

A similar fault array exists south of the Kopeh Dagh (Figure 3), at the northern end of the north-south right-lateral structures within eastern Iran, where these faults die out and are replaced by left-lateral faults that appear to be rotating clockwise about vertical axes (Dasht-e Bayaz and Doruneh; Jackson and McKenzie, 1984; Walker and Jackson, 2004). The slip along the Deh Shir, Anar and Kuh Bahnan faults further south again (Figure 3) may be another example of this behaviour (Walker and Jackson, 2004) and not simply related to the eastern margin of the collision zone (Meyer and Le Dortz, 2007). This explanation has the advantage that such faults are well within the interior of Iran, and so seem poorly located to contribute to shear resulting from the contrast with Afghanistan beyond the collision zone. At the far northwest of Iran and in easternmost Turkey a similar right-lateral fault array is active and allows for shortening within the tip of the Arabian promontory (Copley and Jackson, 2006). Other right-lateral faults trend NNE-SSW or NW-SE across central Iran (e.g. Kashan, Indes). There is limited seismicity on some of these (Figure 2), but little indication that they contribute much to the overall strain pattern at present.

Deformation in the Greater Caucasus represents the northern component of the collision zone at present. Initial uplift in the range may be as old as Late Eocene (Vincent et al., 2007), such that this range carries a longer record of compressional deformation than most parts of the collision zone. Attention has focused on range-parallel thrusts, held responsible for a present-day convergence rate of ~10 mm/yr across it (Reilinger et al. 2006). However, there are oblique features within or close to

421 the Greater Caucasus that look like fault zones at high angles to the overall structural
422 trend. In particular, several folds terminate along NW-SE lines, just inland of the
423 Caspian shoreline (Figure 3). Other structural breaks have the same orientation in the
424 same region. No offsets are identifiable in the exposed geology, so that it is uncertain
425 what these trends mean.
426
427 **Transfer zones and tear faults**
428 A textbook explanation for strike-slip faults within zones of compressional
429 deformation is that they link along-strike sections of the thrusts, either where the latter
430 die out laterally and strain needs to be relayed to another structure, or because it
431 would be mechanically unfeasible to move the thrust sheets if they were too long.
432 Such strike-slip faults are known as tear faults, or transfer faults. They have not been
433 highlighted within the active fold and thrust belts of the Arabia-Eurasia collision. In
434 part this may relate to the blind nature of many thrusts within the Zagros, Alborz,
435 Caucasus and Kopeh Dagh: thrust earthquakes do not typically rupture to the surface
436 through the thick sedimentary cover of these ranges. (This is in contrast to many of
437 the longer strike-slip faults, where earthquake magnitudes can be higher, and surface
438 ruptures are common for the larger events).
439
440 Transfer zones are present on larger scales, although there is potential overlap with
441 some of the other kinematic roles defined in this paper (Figure 4). The Zagros Simple
442 Folded Zone is cut by NNW-SSE or NE-SE trending right-lateral faults such as
443 Kazerun and Sabz Pushan (Figure 8). These have offsets of a few to a few tens of
444 kilometres. Higher estimates, based on range-wide structural and geomorphic
445 correlations (Berberian, 1995) are not confirmed by local studies (Authemayou et al.,

2006). Talebian and Jackson (2004) related these faults to the strike-slip deformation present along the MRF, and the need for lengthening along the Simple Folded Zone as a result of this slip. This is the same style of behaviour as the rotating fault arrays described in the previous section. However, predicted anti-clockwise rotations have not been detected palaeomagnetically (Aubourg et al., 2008). Blanc et al. (2003) noted that the strain partitioning in the NW Zagros does not occur in the east, where folds and thrusts are aligned roughly east-west, orthogonal to the convergence vector, with no strike-slip equivalent to the motion of the MRF. The strike-slip faults within the Simple Folded Zone act to link the zones of strain partitioning and no strain partitioning; individual folds cut by the strike-slip faults also change orientation across them, becoming more east-west further east.

Another scale of transfer behaviour occurs at the western side of the Alborz, where the north-south right-lateral Sangavar Fault (Berberian and Yeats, 1999) links the Alborz to the folds and thrusts in the Talesh (Talysh) range to the north (Figure 9). The arcuate and highly three dimensional nature of the structure in this part of the collision zone relates to the rigid basement of the South Caspian Basin, which underthrusts the Talesh to its west on very gently-dipping thrusts (Jackson et al., 2002). This is superimposed on a component of the regional north-south convergence, such that the overall kinematics appear highly variable in this region (Masson et al., 2006), despite the remarkable consistency in the velocity field with respect to Eurasia (Figure 9).. Deformation at the southeast corner of the collision zone is similarly complex, where the eastern Zagros abuts the Makran accretionary prism (Regard et al., 2005; Bayer et al., 2006).

Discussion

The examples described above demonstrate the different roles that strike-slip faults can play in one timeframe of one collision zone. Some generalities are possible. Strike-slip faults form the boundaries of major deformation zones, where these involve translation rather than convergence or extension. Strain partitioning involves strike-slip faults acting in concert with adjacent, parallel thrusts to achieve the overall convergence vector required by far field conditions. “Far field” mainly means the overall plate convergence zone, but can be rigid blocks moving within it, such as the South Caspian basement. Such partitioning produces the potential for the mis-interpretation of strike-slip faults as tectonic escape structures. Tectonic escape is the valid interpretation for the NAF and EAF, where independent estimates of the regional velocity field confirm the westwards transport of Anatolia with respect to both Arabia and Eurasia. This is not the case for central Iran, where strike-slip faults along the Alborz and Zagros ranges work with parallel thrusts to produce oblique convergence across each range. Geoscientists typically think of thrusts as the predominant structures in orogens, with mountain building as the result. En echelon right-lateral strike-slip faults within Iran show the potential for rotating arrays to achieve plate convergence, without crustal thickening. Such arrays are found both within areas of active thickening (Zagros, Kopeh Dagh, and, possibly, the Greater Caucasus), but also within the Turkish-Iranian plateau, where crustal thickening has ceased. In the latter case, the strike-slip mechanism for convergence has the advantage that it does not require work against gravity, which is important in areas of thickened and/or elevated crust where buoyancy forces oppose crustal thickening. A textbook explanation for strike-slip faults within fold and thrust belts is that they link individual thrusts, and ensure the continuity of strain across large regions. Such features have not

been emphasised to date within the Arabia-Eurasia collision zone, but this may be because many thrusts in actively thickening areas are blind. Larger transfer zones exist, linking entire fold and thrust belts such as the western Alborz and southern Talesh (Figure 9).

In Woodcock's (1986) review of strike-slip faults at plate boundaries, all of the faults described in this paper would fall in the type "Indent-linked strike-slip fault", with the exception of the collision zone boundary faults which partly equate to the "Boundary transform" type. The kinematics of the faults within the Arabia-Eurasia collision, and interpretations on the roles they play in plate convergence, permit a more specific analysis. The five categories listed here (collision zone boundaries, tectonic escape structures, strain partitioning elements, shortening arrays and transfer zones; Figure 3) are not meant to be rigid. No doubt future studies will allow further refinement. The different kinematic roles are not necessarily mutually exclusive. Strike-slip faults in the Zagros link the western and eastern parts of this fold and thrust belt, but also contribute a small amount of shortening across the range (Figure 8).

In recent years there has been a debate as to whether continental deformation is best described by continuum models (where the emphasis is on the smoothness of the velocity field; England and Molnar, 2005), or a rigid block model (where the role of individual fault zones is paramount, and a quasi plate tectonic approach to the kinematics is valid; Thatcher, 2007). The Arabia-Eurasia collision has been involved in this debate, because of the availability of GPS- and seismicity data on its deformation. Reilinger et al. (2006) modelled the behaviour of the collision zone as a series of blocks, which collectively satisfied the overall velocity field. This approach

involved reducing regions as broad and complex as the Zagros (200-300 km width) to a single boundary. Liu and Bird (2008) performed a finite element analysis of active deformation between eastern Anatolia and Burma, modelling geodetic data, geological fault slip rates and seismic moment tensor orientations. They showed that throughout the entire collision zone deformation was distributed, with only a few embedded rigid blocks, such as the South Caspian and Black Sea basins. These have para-oceanic basement distinct from the surrounding continental crust. The derived anelastic strain rate (0.7% per Ma) across the collision zone, apart from these rare blocks, is inconsistent with a rigid microplate model.

The two approaches outlined above produce radically different results. Each is correct in the technical sense that the data are properly handled in the framework of the model parameters. As Thatcher (2007) noted, the transition between the two end member behaviours is blurred: as fault number increases, block size decreases. The important question is, which is the more realistic model of continental behaviour, given the way faulting is distributed across the continental crust in the active examples we have available for study? In this context it is not only the number of fault zones within the Arabia-Eurasia collision that is notable, but their ability to rotate, reverse, accelerate or die within geologically short length- and timescales. Such mobility indicates a distributed model is the more useful way of understanding the deformation, rather than reduction to a small number of rigid microplates. Most of this review has focused on active or at least late Quaternary deformation, because of the wealth of data available for fault slip rates on these timescales. But a satisfactory description of how deformation occurs within the continents may only appear when we have enough data on the pre-neotectonic kinematics. To apply the phrase Brian

546 Windley has made famous, their behaviour cannot be summarised by a snapshot, the
547 key lies in how the continents evolve.
548
549 **Acknowledgements**
550 It is a pleasure to acknowledge and thank Brian Windley for his support and guidance
551 over the last two decades. I am also grateful to the Geological Survey of Iran and the
552 Geology Institute, Azerbaijan Academy of Sciences, for their collaborations on the
553 Arabia-Eurasia collision. The data and ideas reviewed in this paper draw heavily on
554 numerous conversations over the years with James Jackson and Richard Walker, and
555 their insightful papers on the active tectonics of Iran.
556
557

558 **References**

559

560 Allen, M., Jackson, J. & Walker, R. 2004. Late Cenozoic reorganization of the
561 Arabia-Eurasia collision and the comparison of short-term and long-term
562 deformation rates. *Tectonics,* **23**, TC2008, doi: 10.1029/2003TC001530.
563 Allen, M. B. & Armstrong, H. A. 2008. Arabia-Eurasia collision and the forcing of
564 mid Cenozoic global cooling. *Palaeogeography Palaeoclimatology*
565 *Palaeoecology,* **265**, 52-58.
566 Allen, M. B., Ghassemi, M. R., Shahrabi, M. & Qorashi, M. 2003. Accommodation of
567 late Cenozoic oblique shortening in the Alborz range, northern Iran. *Journal of*
568 *Structural Geology,* **25**, 659-672.
569 Allen, M. B., Walker, R., Jackson, J., Blanc, E. J.-P., Talebian, M. & Ghassemi, M. R.
570 2006. Contrasting styles of convergence in the Arabia-Eurasia collision: Why
571 escape tectonics does not occur in Iran. *In:* Dilek, Y. & Pavlides, S. (eds)
572 *Postcollisional tectonics and magmatism in the Mediterranean region and*
573 *Asia.* Geological Society of America, Special Paper, **409**, 579-589.
574 Armijo, R., Meyer, B., Hubert, A. & Barka, A. 1999. Westward propagation of the
575 North Anatolian fault into the northern Aegean: Timing and kinematics.
576 *Geology,* **27**, 267-270.
577 Aubourg, C., Smith, B., Bakhtari, H. R., Guya, N. & Eshraghi, A. 2008. Tertiary
578 block rotations in the Fars Arc (Zagros, Iran). *Geophysical Journal*
579 *International,* **173**, 659-673.
580 Authemayou, C., Chardon, D., Bellier, O., Malekzadeh, Z., Shabanian, E. & Abbassi,
581 M. R. 2006. Late Cenozoic partitioning of oblique plate convergence in the

582 Zagros fold-and-thrust belt (Iran). *Tectonics,* **25**, TC3002, doi
583 10.1029/2005tc001860.
584 Axen, G. J., Lam, P. S., Grove, M., Stockli, D. F. & Hassanzadeh, J. 2001.
585 Exhumation of the west-central Alborz Mountains, Iran, Caspian subsidence,
586 and collision-related tectonics. *Geology*, **29**, 559-562.
587 Bachmanov, D. M., Trifonov, V. G., Hessami, K. T., Kozhurin, A. I., Ivanova, T. P.,
588 Rogozhin, E. A., Hademi, M. C. & Jamali, F. H. 2004. Active faults in the
589 Zagros and central Iran. *Tectonophysics,* **380**, 221-241.
590 Barka, A. A. & Hancock, P. L. 1984. Neotectonic deformation patterns in the convex-
591 northwards arc of the North Anatolian fault. *In:* Dixon, J. E. & Robertson, A.
592 H. F. (eds) *The Geological Evolution of the Eastern Mediterranean*.
593 Geological Society, London, Special Publications, **17**, 763-773.
594 Bayer, R., Chery, J., Tatar, M., Vernant, P., Abbassi, M., Masson, F., Nilforoushan,
595 E., Doerflinger, E., Regard, V. & Bellier, O. 2006. Active deformation in
596 Zagros-Makran transition zone inferred from GPS measurements. *Geophysical*
597 *Journal International*, **165**, 373-381.
598 Berberian, M. 1995. Master "blind" thrust faults hidden under the Zagros folds: active
599 basement tectonics and surface morphotectonics. *Tectonophysics,* **241**, 193-
600 224.
601 Berberian, M. & Yeats, R. S. 1999. Patterns of historical earthquake rupture in the
602 Iranian plateau. *Bulletin of the Seismological Society of America,* **89**, 120-139.
603 Beydoun, Z. R., Hughes Clarke, M. W. & Stoneley, R. 1992. Petroleum in the Zagros
604 Basin: a late Tertiary foreland basin overprinted onto the outer edge of a vast
605 hydrocarbon-rich Paleozoic-Mesozoic passive-margin shelf. *In:* MacQueen, R.

& Leckie, D. (eds) *Foreland Basins and Foldbelts*. AAPG Memoir **55**, 309-339.

Blanc, E. J.-P., Allen, M. B., Inger, S. & Hassani, H. 2003. Structural styles in the Zagros Simple Folded Zone, Iran. *Journal of the Geological Society, London* **160**, 400-412.

Bozkurt, E. 2001. Neotectonics of Turkey - a synthesis. *Geodinamica Acta,* **14**, 3-30.

Copley, A. & Jackson, J. 2006. Active tectonics of the Turkish-Iranian Plateau. *Tectonics,* **25**, doi: 10.1029/2005TC001096.

Coskun, B. 2000. North Anatolian Fault-Saros Gulf relationships and their relevance to hydrocarbon exploration, northern Aegean Sea, Turkey. *Marine and Petroleum Geology,* **17**, 751-772.

de Voogd, B., Truffert, C., Chamotrooke, N., Huchon, P., Lallemant, S. & Lepichon, X. 1992. 2-ship deep seismic-soundings in the basins of the eastern Mediterranean Sea (Pasiphae cruise). *Geophysical Journal International,* **109**, 536-552.

Devlin, W., Cogswell, J., Gaskins, G., Isaksen, G., Pitcher, D., Puls, D., Stanley, K. & Wall, G. 1999. South Caspian Basin: young, cool, and full of promise. *GSA Today,* **9**, 1-9.

Dewey, J. F., Hempton, M. R., Kidd, W. S. F., Saroglu, F. & Şengör, A. M. C. 1986. Shortening of continental lithosphere: the neotectonics of Eastern Anatolia - a young collision zone. *In:* Coward, M. & Ries, A. (eds) *Collision Tectonics*. Geological Society, London, Special Publications, **19**, 3-36.

Engdahl, E. R., van der Hilst, R. & Buland, R. 1998. Global teleseismic earthquake relocation with improved travel times and procedures for depth determination. *Bulletin of the Seismological Society of America,* **88**, 722-743.

631 England, P. & Molnar, P. 2005. Late Quaternary to decadal velocity fields in Asia.
632 *Journal Of Geophysical Research-Solid Earth,* **110**(B12), doi:
633 10.1029/2004JB003541.
634 Eyal, M., Eyal, Y., Bartov, Y. & Steinitz, G. 1981. The tectonic development of the
635 western margin of the Gulf of Elat, Aqaba, rift. *Tectonophysic,s* **80**, 39-66.
636 Ferry, M., Meghraoui, M., Abou Karaki, N., Al-Taj, M., Amoush, H., Al-Dhaisat, S.
637 & Barjous, M. 2007. A 48-kyr-long slip rate history for the Jordan Valley
638 segment of the Dead Sea Fault. *Earth and Planetary Science Letters,* **260**,
639 394-406.
640 Garfunkel, Z. 1981. Internal structure of the Dead Sea leaky transform (rift) in
641 relation to plate kinematics. *Tectonophysics,* **80**, 81-108.
642 Gomez, F., Karam, G., Khawlie, M., McClusky, S., Vernant, P., Reilinger, R., Jaafar,
643 R., Tabet, C., Khair, K. & Barazangi, M. 2007. Global Positioning System
644 measurements of strain accumulation and slip transfer through the restraining
645 bend along the Dead Sea fault system in Lebanon. *Geophysical Journal*
646 *International,* **168**, 1021-1028.
647 Guest, B., Stockli, D.F., Grove, M., Axen, G.J., Lam, P.S. & Hassanzadeh, J. 2006a.
648 Thermal histories from the central Alborz Mountains, northern Iran:
649 Implications for the spatial and temporal distribution of deformation in
650 northern Iran. *Geological Society of America Bulletin,* **118**, 1507-1521.
651 Guest, B., Axen, G.J., Lam, P.S. & Hassanzadeh, J. 2006b. Late Cenozoic shortening
652 in the west-central Alborz Mountains, northern Iran, by combined conjugate
653 strike-slip and thin-skinned deformation. *Geosphere,* **2**, 35-52.

654 Hollingsworth, J., Jackson, J., Walker, R., Gheitanchi, M. R. & Bolourchi, M. J. 2006.
655 Strike-slip faulting, rotation, and along-strike elongation in the Kopeh Dagh
656 mountains, NE Iran. *Geophysical Journal International,* **166**, 1161-1177.
657 Hollingsworth, J., Jackson, J., Walker, R., & Nazari, H. 2008. Extrusion tectonics and
658 subduction in the eastern South Caspian region since 10 Ma. *Geology*, **36**,
659 763-766.
660 Homke, S., Vergés, J., Garcés, M., Emami, H. & Karpuz, R. 2004.
661 Magnetostratigraphy of Miocene–Pliocene Zagros foreland deposits in the
662 front of the Push-e Kush Arc (Lurestan Province, Iran). *Earth and Planetary*
663 *Science Letters,* **225**, 397-410.
664 Jackson, J. 1992. Partitioning of strike-slip and convergent motion between Eurasia
665 and Arabia in eastern Turkey and the Caucasus. *Journal of Geophysical*
666 *Research,* **97**, 12471-12479.
667 Jackson, J. 2001. Living with earthquakes: Know your faults. *Journal of Earthquake*
668 *Engineering,* **5**, 5-123.
669 Jackson, J., Haines, A. J. & Holt, W. E. 1995. The accommodation of Arabia-Eurasia
670 plate convergence in Iran. *Journal of Geophysical Research,* **100**, 15205-
671 15209.
672 Jackson, J. & McKenzie, D. 1984. Active tectonics of the Alpine-Himalayan belt
673 between western Turkey and Pakistan. *Geophysical Journal of the Royal*
674 *Astronomical Society*, **77**, 185-264.
675 Jackson, J., Priestley, K., Allen, M. & Berberian, M. 2002. Active tectonics of the
676 South Caspian Basin. *Geophysical Journal International,* **148**, 214-245.
677 Jaffey, N. & Robertson, A. H. F. 2001. New sedimentological and structural data from
678 the Ecemis Fault Zone, southern Turkey: implications for its timing and offset

679 and the Cenozoic tectonic escape of Anatolia. *Journal of the Geological*
680 *Society*, **158**, 367-378.
681 Jolivet, L. & Faccenna, C. 2000. Mediterranean extension and the Africa-Eurasia
682 collision. *Tectonics,* **19**, 1095-1106.
683 Keskin, M., Pearce, J. A. & Mitchell, J. G. 1998. Volcano-stratigraphy and
684 geochemistry of collision-related volcanism on the Erzurum-Kars Plateau,
685 northeastern Turkey. *Journal of Volcanology and Geothermal Research* **85**,
686 355-404.
687 Kheirkhah, M., Allen, M. B. & Emami, M. 2009. Quaternary syn-collision
688 magmatism from the Iran/Turkey borderlands. *Journal of Volcanology and*
689 *Geothermal Research* **182**, 1-12.
690 Klinger, Y., Avouac, J. P., Abou Karaki, N., Dorbath, L., Bourles, D. & Reyss, J. L.
691 2000. Slip rate on the Dead Sea transform fault in northern Araba valley
692 (Jordan). *Geophysics Journal International,* **142**, 755-768.
693 Kocyigit, A. & Beyhan, A. 1998. A new intracontinental transcurrent structure: the
694 Central Anatolian Fault Zone, Turkey. *Tectonophysics,* **284**, 317-336.
695 Kocyigit, A., Yilmaz, A., Adamia, S. & Kuloshvili, S. 2001. Neotectonics of East
696 Anatolian Plateau (Turkey) and Lesser Caucasus: implication for transition
697 from thrusting to strike-slip faulting. *Geodinamica Acta,* **14**, 177-195.
698 Liu, Z. & Bird, P. 2008. Kinematic modelling of neotectonics in the Persia-Tibet-
699 Burma orogen. *Geophysical Journal International*, **172**, 779-797.
700 Lyberis, N. & Manby, G. 1999. Oblique to orthogonal convergence across the Turan
701 Block in the Post-Miocene. *Bulletin of the American Association of Petroleum*
702 *Geologists,* **83**, 1135-1160.

703 Lyberis, N., Yurur, T., Chorowicz, J., Kasapoglu, E. & Gundogdu, N. 1992. The East
704 Anatolian Fault: an oblique collisional belt. *Tectonophysics,* **204**, 1-15.
705 Mangino, S. & Priestley, K. 1998. The crustal structure of the southern Caspian
706 region. *Geophysical Journal International,* **133**, 630-648.
707 Mann, P. 2007. Global catalogue, classififcation and tectonic origins of restraining-
708 and releasing bends on active and ancient strike-slip fault systems. *In:*
709 Cunningham, W.D. & Mann, P. (eds) *Tectonics of Strike-slip restraining and*
710 *releasing bends.* Geological Society, London, Special Publications, **290**, 13-
711 142.
712 Manspeizer, W. 1985. The Dead Sea Rift: impact of climate and tectonism on
713 Pleistocene and Holocene sedimentation. *In:* Biddle, K. & Christie-Blick, N.
714 (eds) *Strike-slip Deformation, Basin Formation and Sedimentation.* Society of
715 Economic Paleontolgists and Mineralogists, Special Publication, **37**, 143-158.
716 Masson, F., Djamour, Y., Van Gorp, S., Chery, J., Tatar, M., Tavakoli, F., Nankali, H.
717 & Vernant, P. 2006. Extension in NW Iran driven by the motion of the south
718 Caspian basin. *Earth and Planetary Science Letters* **252**, 180-188.
719 McClusky, S. & 27 others, 2000. Global Positioning System constraints on plate
720 kinematics and dynamics in the eastern Mediterranean and Caucasus. *Journal*
721 *of Geophysical Researc,h* **105**, 5695-5719.
722 McClusky, S., Reilinger, R., Mahmoud, S., Ben Sari, D. & Tealeb, A. 2003. GPS
723 constraints on Africa (Nubia) and Arabia plate motions. *Geophysical Journal*
724 *International,* **155**, 126-138.
725 McKenzie, D. P. 1972. Active tectonics of the Mediterranean region. *Geophysical*
726 *Journal of the Royal Astronomical Society,* **30**, 109-185.

McQuarrie, N. 2004. Crustal scale geometry of the Zagros fold-thrust belt, Iran. *Journal of Structural Geology,* **26**, 519-535.

McQuarrie, N., Stock, J. M., Verdel, C. & Wernicke, B. 2003. Cenozoic evolution of Neotethys and implications for the causes of plate motions. *Geophysical Research Letters,* **30**, 2036, doi: 10.1029/2003GL017992.

Meyer, B. & Le Dortz, K. 2007. Strike-slip kinematics in Central and Eastern Iran: Estimating fault slip-rates averaged over the Holocene. *Tectonics,* **26**, Tc5009, doi: 10.1029/2006tc002073.

Meyer, B., Mouthereau, F., Lacombe, O. & Agard, P. 2006. Evidence of Quaternary activity along the Deshir Fault: implication for the tertiary tectonics of central Iran. *Geophysical Journal International,* **164**, 192-201.

Pearce, J. A., Bender, J. F., Delong, S. E., Kidd, W. S. F., Low, P. J., Guner, Y., Sargolu, F., Yilmaz, Y., Moorbath, S. & Mitchell, J. G. 1990. Genesis of collision volcanism in eastern Anatolia, Turkey. *Journal of Volcanology and Geothermal Research* **44**, 189-229.

Quennell, A. M. 1958. The structure and evolution of the Dead Sea rift. *Quarterly Journal of the Geological Society,* **64**, 1-24.

Regard, V., Bellier, O., Thomas, J.C., Bourles, D., Bonnet, S., Abbassi, M.R., Braucher, R., Mercier, J., Shabanian, E., Soleymani, S. & Feghhi, K. 2005. Cumulative right-lateral fault slip rate across the Zagros-Makran transfer zone: role of the Minab-Zendan fault system in accommodating Arabia-Eurasia convergence in southeast Iran. *Geophysical Journal International,* **162,** 177-203.

Reilinger, R., McClusky, S., Vernant, P., Lawrence, S., Ergintav, S., Cakmak, R., Ozener, H., Kadirov, F., Guliev, I., Stepanyan, R., Nadariya, M., Hahubia, G.,

Mahmoud, S., Sakr, K., ArRajehi, A., Paradissis, D., Al-Aydrus, A., Prilepin, M., Guseva, T., Evren, E., Dmitrotsa, A., Filikov, S. V., Gomez, F., Al-Ghazzi, R. & Karam, G. 2006. GPS constraints on continental deformation in the Africa-Arabia-Eurasia continental collision zone and implications for the dynamics of plate interactions. *Journal of Geophysical Research-Solid Earth,* **111**, B05411 doi: 10.1029/2005JB004051.

Ritz, J. F., Nazari, H., Ghassemi, A., Salamati, R., Shafei, A., Solaymani, S. & Vernant, P. 2006. Active transtension inside central Alborz: A new insight into northern Iran-southern Caspian geodynamics. *Geology,* **34**, 477-480.

Sargolu, F., Emre, O. & Kuscu, I. 1992. The East Anatolian Fault of Turkey. *Annales Tectonicae,* **6**, 99-125.

Sarkarinejad, K., Faghih, A. & Grasernann, B. 2008. Transpressional deformations within the Sanandaj-Sirjan metamorphic belt (Zagros Mountains, Iran). *Journal of Structural Geology,* **30**, 818-826.

Şengör, A. M. C., Altiner, D., Cin, A., Ustaomer, T. & Hsu, K. J. 1988. Origin and assembly of the Tethyside orogenic collage at the expense of Gondwana Land. *In:* Audley-Charles, M. G. & Hallam, A. (eds) *Gondwana and Tethys* Geological Society, London, Special Publications, **37**, 119-181.

Şengör, A. M. C., Tuysuz, O., Imren, C., Sakinc, M., Eyidogan, H., Gorur, G., Le Pichon, X. & Rangin, C. 2005. The North Anatolian Fault: A new look. *Annual Review of Earth and Planetary Sciences,* **33**, 37-112.

Seymen, I. 1975. *Tectonic characteristics of the North Anatolian Fault zone in the Kelkit Valley segment*. Istanbul Teknik Universitesi Maden Fakultesi Yayinlari, Istanbul.

776 Talebian, M. & Jackson, J. 2002. Offset on the Main Recent Fault of NW Iran and
777 implications for the late Cenozoic tectonics of the Arabia-Eurasia collision
778 zone. *Geophysical Journal International,* **150**, 422-439.
779 Talebian, M. & Jackson, J. 2004. A reappraisal of earthquake focal mechanisms and
780 active shortening in the Zagros mountains of Iran. *Geophysical Journal*
781 *International,* **156**, 506-526.
782 Tatar, M., Jackson, J., Hatzfeld, D. & Bergman, E. 2007. The 2004 May 28 Baladeh
783 earthquake (M-w 6.2) in the Alborz, Iran: overthrusting the South Caspian
784 Basin margin, partitioning of oblique convergence and the seismic hazard of
785 Tehran. *Geophysical Journal International,* **170**, 249-261.
786 Thatcher, W. 2007. Microplate model for the present-day deformation of Tibet.
787 *Journal of Geophysical Research-Solid Earth,* **112**, B01401 doi:
788 10.1029/2005jb004244.
789 Tuysuz, O., Barka, A. & Yigitbas, E. 1998. Geology of the Saros graben and its
790 implications for the evolution of the North Anatolian fault in the Ganos-Saros
791 region, northwestern Turkey. *Tectonophysics* **293**, 105-126.
792 Verdel, C., Wernicke, B. P., Ramezani, J., Hassanzadeh, J., Renne, P. R. & Spell, T.
793 L. 2007. Geology and thermochronology of Tertiary Cordilleran-style
794 metamorphic core complexes in the Saghand region of central Iran.
795 *Geological Society of America Bulletin,* **119**, 961-977.
796 Vernant, P., Nilforoushan, F., Chery, J., Bayer, R., Djamour, Y., Masson, F., Nankali,
797 H., Ritz, J. F., Sedighi, M. & Tavakoli, F. 2004b. Deciphering oblique
798 shortening of central Alborz in Iran using geodetic data. *Earth and Planetary*
799 *Science Letters,* **223**, 177-185.

800 Vernant, P., Nilforoushan, F., Hatzfeld, D., Abbassi, M., Vigny, C., Masson, F.,
801 Nankali, H., Martinod, J., Ashtiani, A., Bayer, R., Tavakoli, F. & Chery, J.
802 2004a. Contemporary crustal deformation and plate kinematics in Middle East
803 constrained by GPS measurements in Iran and northern Iran. *Geophysical*
804 *Journal International,* **157**, 381-398.
805 Vincent, S. J., Allen, M. B., Ismail-Zadeh, A. D., Flecker, R., Foland, K. A. &
806 Simmons, M. D. 2005. Insights from the Talysh of Azerbaijan into the
807 Paleogene evolution of the South Caspian region. *Bulletin of the Geological*
808 *Society of America,* **117**, 1513-1533.
809 Vincent, S. J., Morton, A. C., Carter, A., Gibbs, S. & Barabadze, T. G. 2007.
810 Oligocene uplift of the Western Greater Caucasus: an effect of initial Arabia-
811 Eurasia collision. *Terra Nova,* **19**, 160-166.
812 Walker, R. & Jackson, J. 2004. Active tectonics and late Cenozoic strain distribution
813 in central and eastern Iran. *Tectonics,* **23**, TC5010; doi:
814 10.1029/2003TC001529.
815 Walker, R. T., Bergman, E., Jackson, J., Ghorashi, M. & Talebian, M. 2005. The 2002
816 June 22 Changureh (Avaj) earthquake in Qazvin province, northwest Iran:
817 epicentral relocation, source parameters, surface deformation and
818 geomorphology. *Geophysical Journal International,* **160**, 707-720.
819 Walker, R. T., Gans, P., Allen, M. B., Jackson, J., Khatib, M., Marsh, N. &
820 Zarrinkoub, M. 2009. Late Cenozoic volcanism and rates of active faulting in
821 eastern Iran. *Geophyical Journal International* **177**, 783-805.
822 Westaway, R. 1994. Present-day kinematics of the Middle-East and Eastern
823 Mediterranean. *Journal of Geophysical Research,* **99**, 12071-12090.

824 Westaway, R. 1999. Comment on "A new intracontinental transcurrent structure: the
825 Central Anatolian Fault Zone, Turkey" by A. Kocyigit and A. Beyhan.
826 *Tectonophysics,* **314**, 469-479.
827 Westaway, R. & Arger, J. 1996. The Golbasi basin, southeastern Turkey: A complex
828 discontinuity in a major strike-slip fault zone. *Journal of the Geological*
829 *Society,* **153**, 729-743.
830 Westaway, R. & Arger, J. 2001. Kinematics of the Malatya-Ovacik fault zone.
831 *Geodinamica Acta,* **14**, 103-131.
832 Westaway, R., Demir, T., Seyrek, A. & Beck, A. 2006. Kinematics of active left-
833 lateral faulting in SE Turkey from offset Pleistocene river gorges: improved
834 constraint on the rate and history of relative motion between the Turkish and
835 Arabian plates. *Journal of the Geological Society,* **163**, 149-164.
836 Woodcock, N. H. 1986. The role of strike-slip fault systems at plate boundaries.
837 *Philosophical Transactions of the Royal Society of London Series A-*
838 *Mathematical Physical And Engineering Sciences,* **317,** 13-29.
839 Zanchi, A., Berra, F., Mattei, M., Ghassemi, M. R. & Sabouri, J. 2006. Inversion
840 tectonics in central Alborz, Iran. *Journal of Structural Geology,* **28**, 2023-
841 2037.
842

Figures

Figure 1. GPS-derived velocity field of the Arabia-Eurasia collision, with respect to stable Eurasia. The dashed line is the Bitlis-Zagros suture. Compiled from McClusky et al. (2000) and Vernant et al. (2004a).

Figure 2. Seismicity of the Arabia-Eurasia collision zone (from Allen et al., 2006). Small dots are epicentres from the catalogue of Engdahl et al. (1998). Focal mechanisms are from the following sources. Black: Waveform modelled, from Jackson (2001) and references therein, with additional events from Talebian et al. (2004) and Walker et al. (2005). Dark gray: Best-double-couple CMT solutions from the Harvard catalogue (http://www.seismology/harvard.edu/CMTsearch.html) for earthquakes with depth ≤ 35 km, Mw ≥ 5.5 and double-couple component ≥ 70%, in the interval 1977-2002. Light Gray: First motion solutions from Jackson and McKenzie (1984). Earthquakes deeper than 35 km associated with the subduction zones in the Makran, South Caspian and Hellenic Trench have been omitted.

Figure 3. Major active strike-slip fault zones within the Arabia-Eurasia collision zone. Derived from Allen et al. (2006) (Iran), Copley and Jackson (2006) (NW Iran), Allen et al. (2003) (N Iran), Bozkurt (2001) (central and NW Turkey), Kocyigit et al. (2001) (eastern Turkey). Activity on strike-slip faults in much of Anatolia is debated (e.g. Kocyigit and Beyhan, 1998, and Westaway, 1999), so that the Eskisehir and Central Anatolian faults are marked by dashed lines, and others shown by Bozkurt (2001) and Kocyigit et al. (2001) are not shown at all. The Salanda Fault is in the vicinity of a strike-slip earthquake of 1938 (Jackson and McKenzie, 1984), and so is more confidently assigned as active. Barbed lines show active thrust fronts, schematically.

Thrust zones are typically harder to map as precisely, because many of the active thrusts are blind. White barbs are subduction zones at the margins of the South Caspian Basin and Makran and along the Cypriot and Helenic arcs. Red Sea oceanic spreading is shown schematically by the double line.

Figure 4. Schematised kinematics of a continent-continent collision between plates X and Y, modelled after the Arabia-Eurasia collision and showing westward tectonic escape of block Z (i.e. Anatolia) and lateral strike-slip faults at the western and eastern boundary zones. Solid triangles indicate thrusts at the margins of the collision zone; open triangles indicate adjacent subduction zones. Thick black arrows indicate velocities with respect to the stable interior of block Y, with length proportional to velocity. The five roles of strike-slip faults described in this paper are highlighted as follows: (1) Collision zone boundaries – either diffuse or focussed (2) Tectonic escape structures (3) Strain partitioning elements (4) Shortening arrays with vertical axis rotations (5) Transfer zones.

Figure 5. The concept of strain partitioning: A) combined slip on the strike-slip fault and shortening across the adjacent thrust belt produces net convergence oblique to the fault trends – northwards motion of block X with respect to Y. This scenario is similar to the northwest Zagros Simple Folded Zone. B) Strain partitioning where the strike-slip fault system lies within the interior of the thrust zone. This geometry is similar to the Alborz mountains.

Figure 6. Active faults in the Alborz between 51^{o} and 55^{o} E. Left-lateral faulting occurs within the range interior, principally on the Taleghan, Mosha, Firuzkuh, and

Astaneh faults, which collectively form a segmented fault system. Thrusting takes place on inward-dipping faults at both the northern and southern margins of the range. The continuity of the Khazar Fault may be an artefact of Caspian lake highstands bevelling southwards against the bedrock of the range: the thrust is blind. Map derived from Allen et al. (2003), Ritz et al. (2006), Hollingsworth et al. (2008) and analysis of SRTM digital topography; focal mechanisms from Jackson et al. (2002) and Tatar et al. (2007).

Figure 7. Rotating strike-slip arrays acting to produce shortening and along-strike elongation (from Hollingsworth et al., 2006), as seen in the Kopeh Dagh. A) Fault blocks have initial width d and angle θ_0 with the deformation zone boundary, across a zone of width W_0. Grey bands represent fold trends, which act as strain markers as the faults and fault blocks are offset and rotated. B) Offset and fault block rotation produces new boundary length D, and angle θ_1, across a width W_1. C) If all fault block rotations are of the same amount, the geometry simplifies to a single triangle with lengths ΣD, Σd and Σs. Measurement of ΣD, Σs, θ_0 and θ_1 allows the original length of the deforming boundary (Σd) to be calculated using the cosine rule.

Figure 8. Active strike-slip faults in the Central Zagros. Several segmented right-lateral faults fan out from the southeastern end of the Main Recent Fault. Fault locations derived from Authemayou et al. (2006) and analysis of SRTM imagery. Focal mechanisms for thrust and strike-slip events in the region are from the Harvard and USGS catalogues (http://neic.usgs.gov/neis/sopar/) for earthquakes with $Mw \geq 5$ and double-couple component $\geq 70\%$, in the interval 1986-2005.

Figure 9. Active faulting in the Talesh and western Alborz mountains, illustrating the role of the right-lateral Sangavar Fault as a transfer fault between the regions. Focal mechanisms from Jackson et al. (2002), with three additional events from the Harvard and USGS catalogues (http://neic.usgs.gov/neis/sopar/) for earthquakes with Mw ≥ 5 and double-couple component ≥ 70%, in the interval 2002-2007. Arrows show GPS-derived velocities with respect to Eurasia, from Masson et al. (2006). These do not change markedly across the region, despite the wide variation in fault strikes and focal mechanisms. The inset is a schematic transfer zone between two thrust belts, modelled on the junction of the Talesh and Alborz ranges. Deformation not only wraps around the rigid basement of block X, but has to accommodate its motion independent of the north-south convergence of larger regions Y and Z. This produces highly arcuate and complex fault geometries, which are unlikely to be stable over long periods.

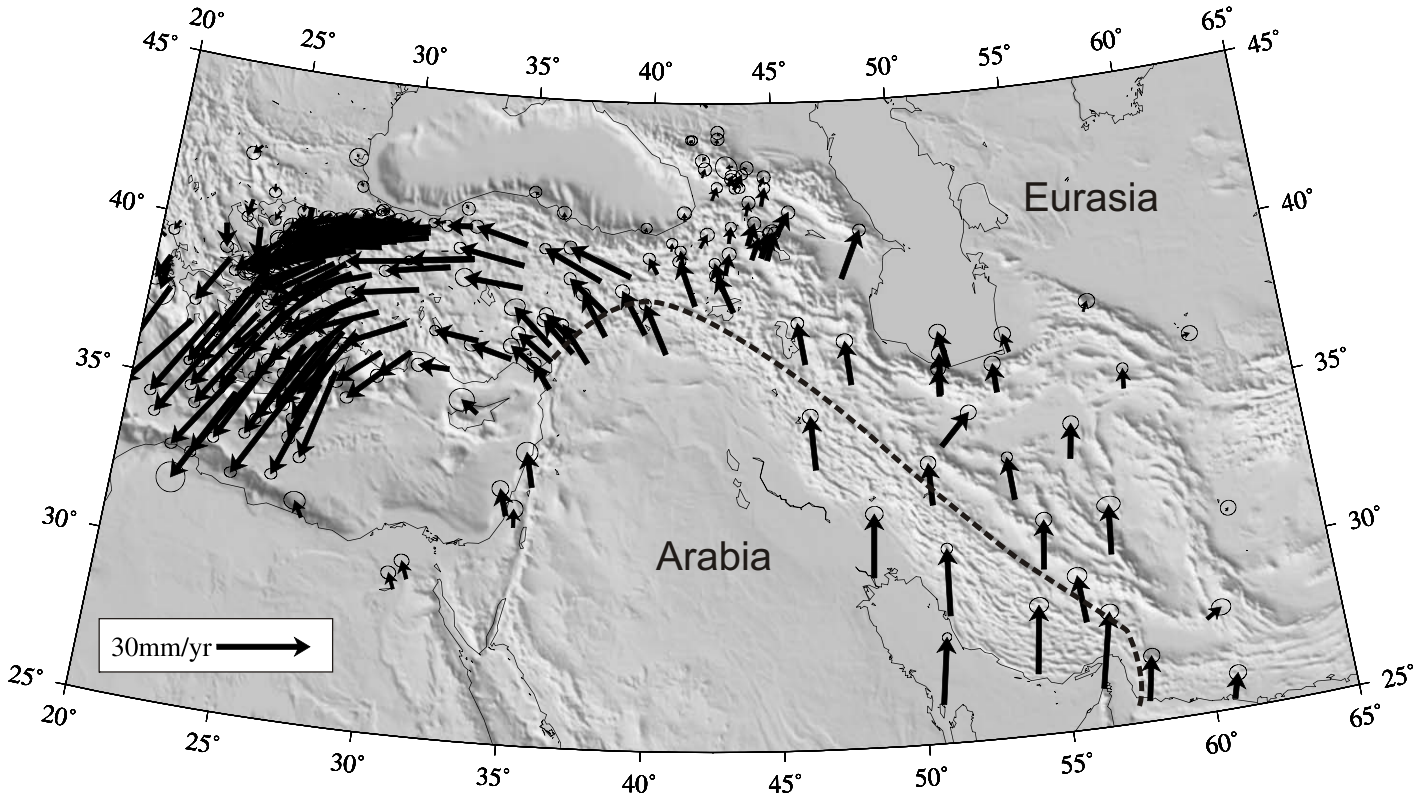

1.

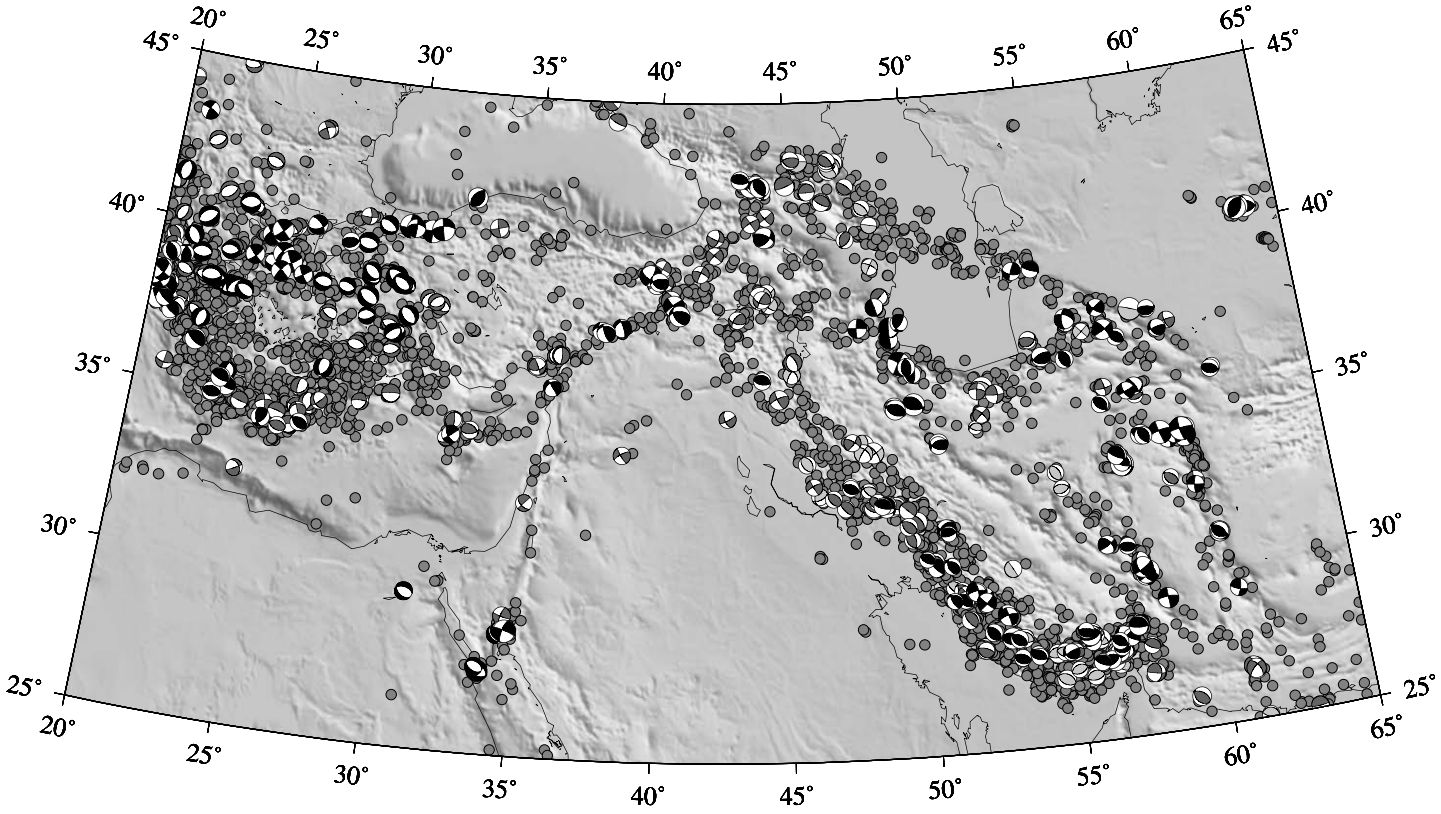

2.

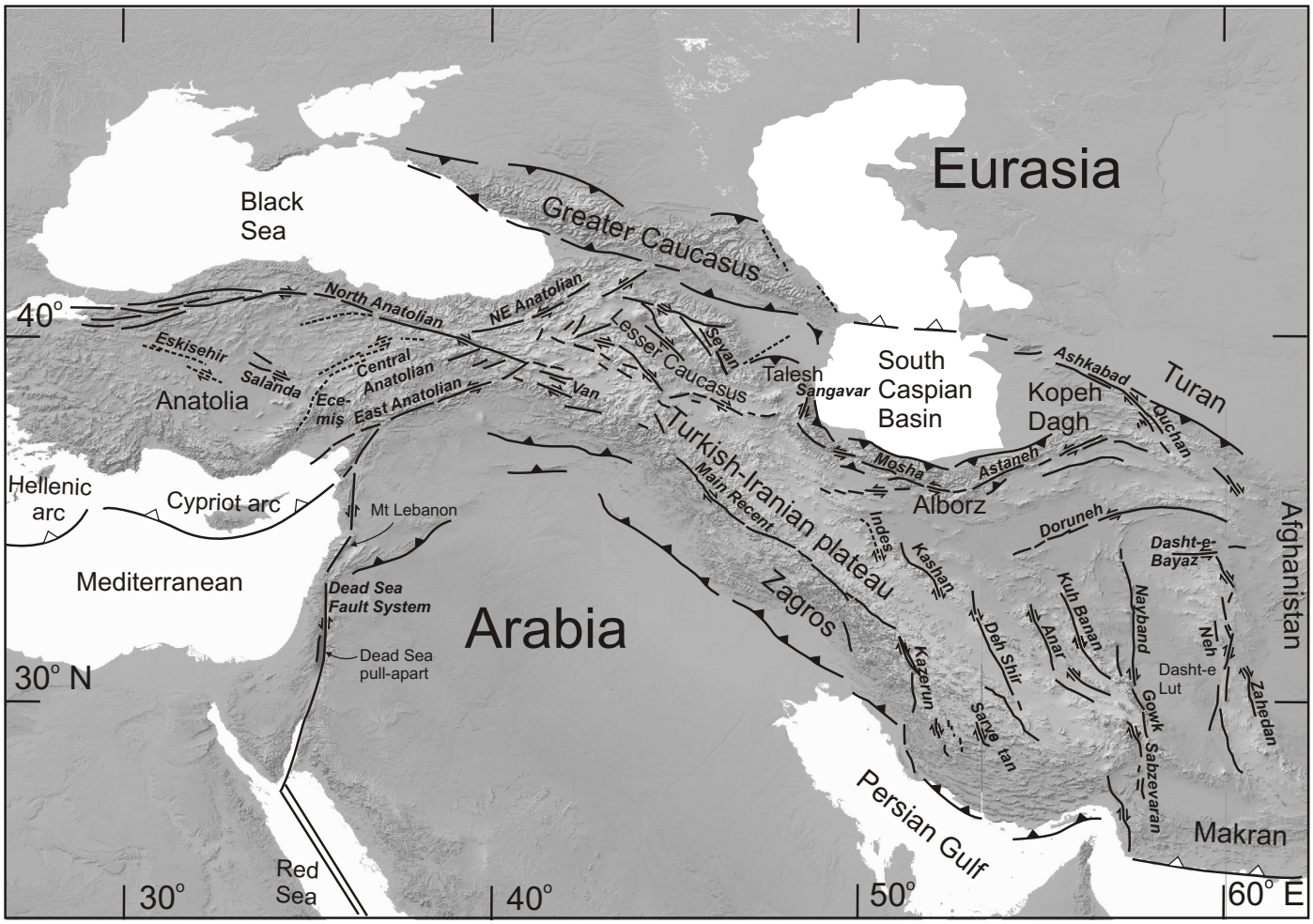
Eurasia
Black Sea
Greater Caucasus
North Anatolian
NE Anatolian
Eskisehir
Salanda
Central Anatolian
Ece-miş
East Anatolian
Anatolia
Lesser Caucasus
Sevan
Talesh
Sangavar
South Caspian Basin
Ashkabad
Turan
Quchan
Kopeh Dagh
Van
Turkish-Iranian plateau
Main Recent
Mosha
Astaneh
Alborz
Doruneh
Afghanistan
Hellenic arc
Cypriot arc
Mt Lebanon
Mediterranean
Dead Sea Fault System
Dead Sea pull-apart
Arabia
Indes
Kashan
Zagros
Dasht-e-Bayaz
Kuh Banan
Nayband
Anar
Deh Shir
Kazerun
Sanandaj
Neh
Dasht-e Lut
Gowk
Sabzevaran
Zahedan
Persian Gulf
Makran
Red Sea
40°
30° N
30°
40°
50°
60° E

3.

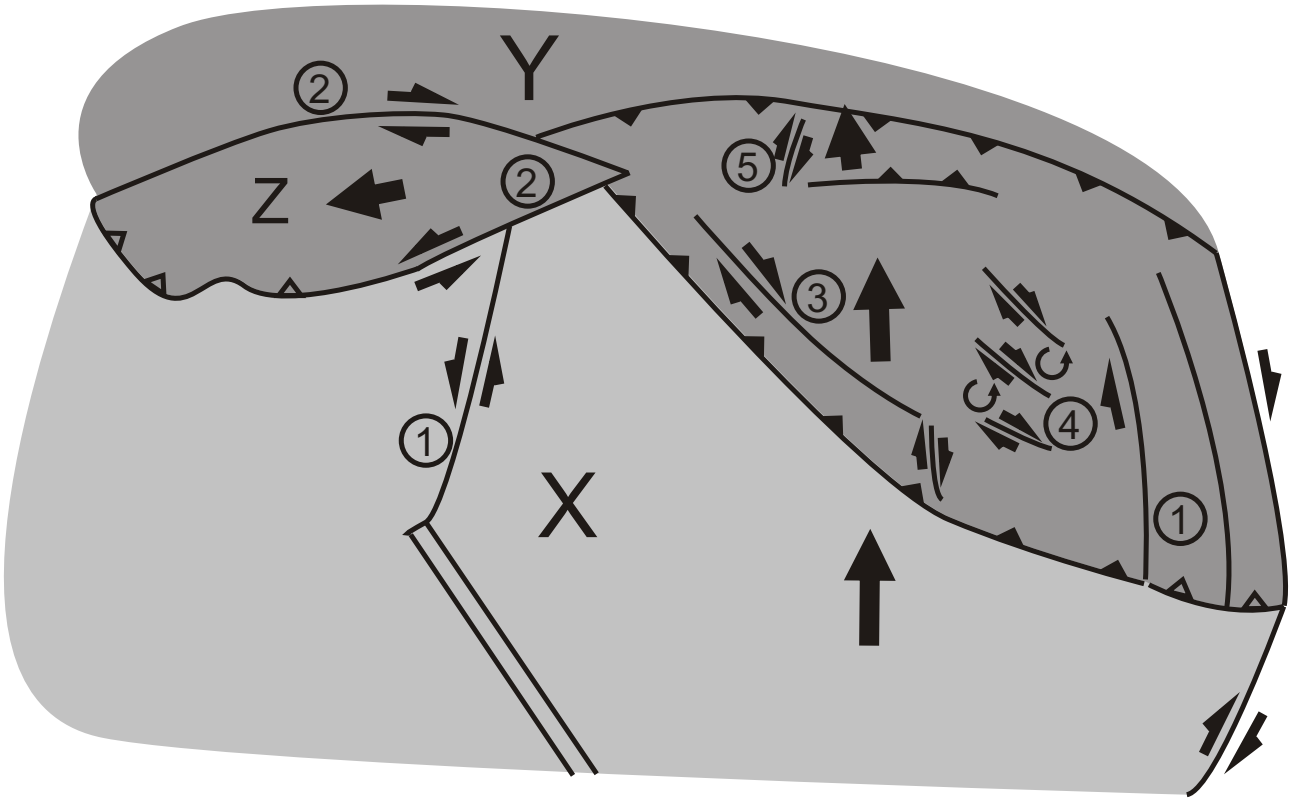

4.

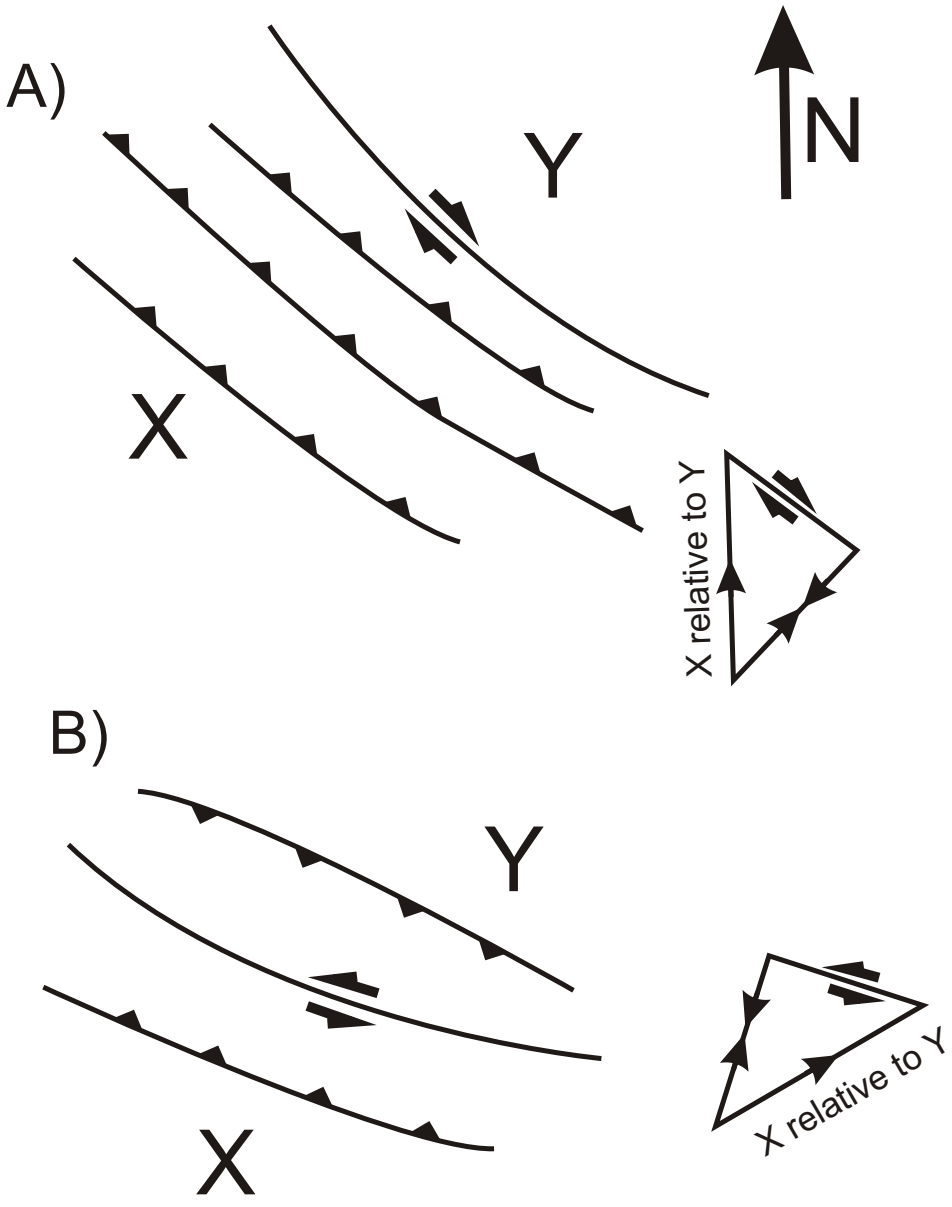

5.

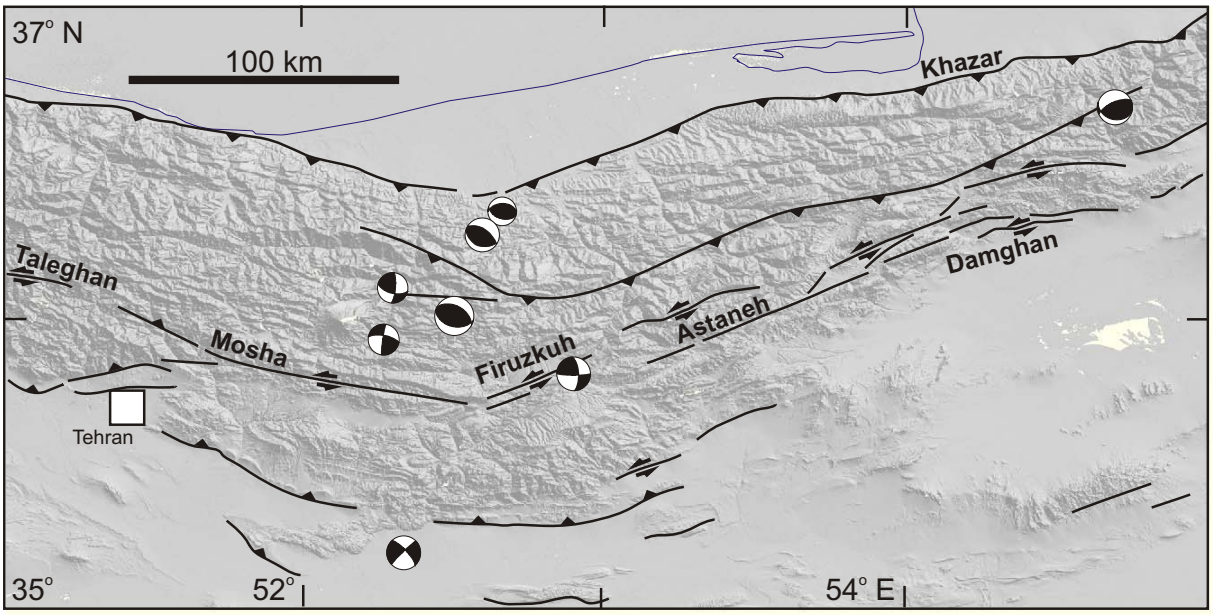
37° N
100 km
Khazar
Taleghan
Mosha
Firuzkuh
Astaneh
Damghan
Tehran
35°
52°
54° E

6.

A)

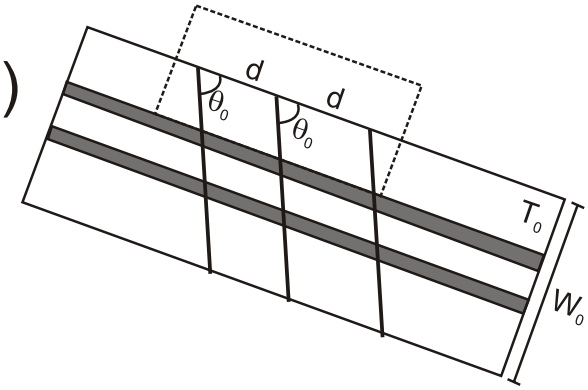
d
d
θ_0
θ_0
T_0
W_0

B)

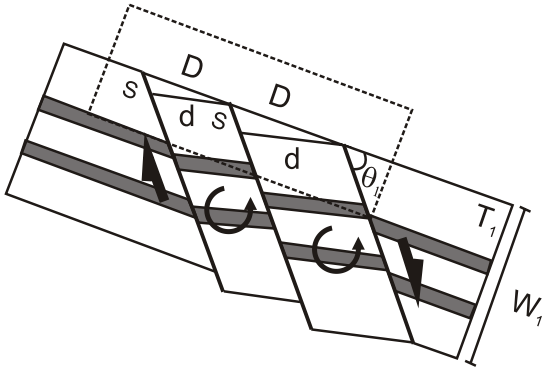
D
D
s
d
s
d
θ_1
T_1
W_1

C)

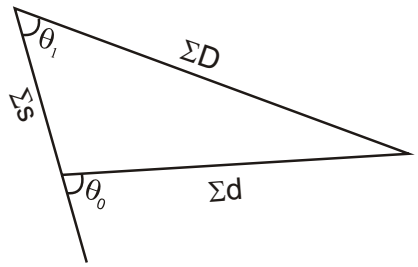
θ_1
ΣD
Σs
θ_0
Σd

7.

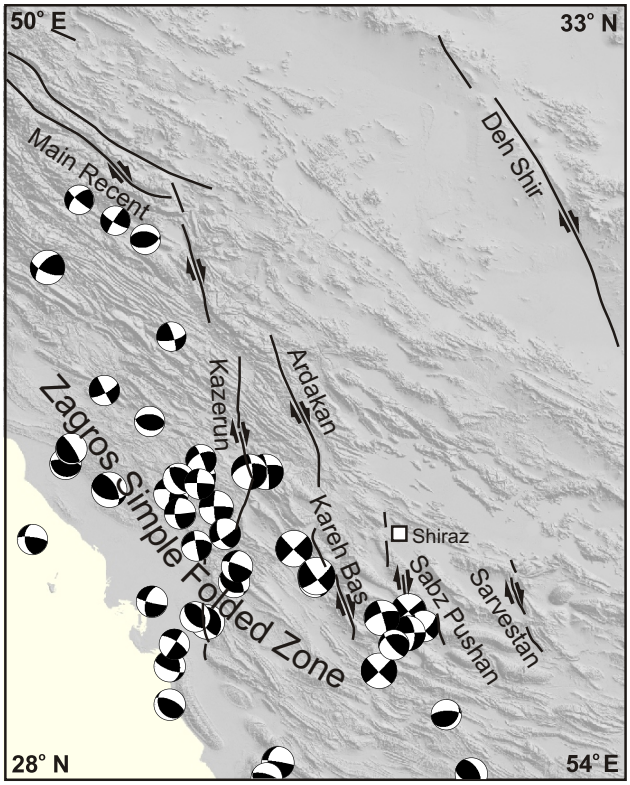
50° E
33° N
Main Recent
Deh Shir
Kazerun
Ardakan
Zagros Simple Folded Zone
Kareh Bas
Shiraz
Sabz Pushan
Sarvestan
28° N
54° E

8.

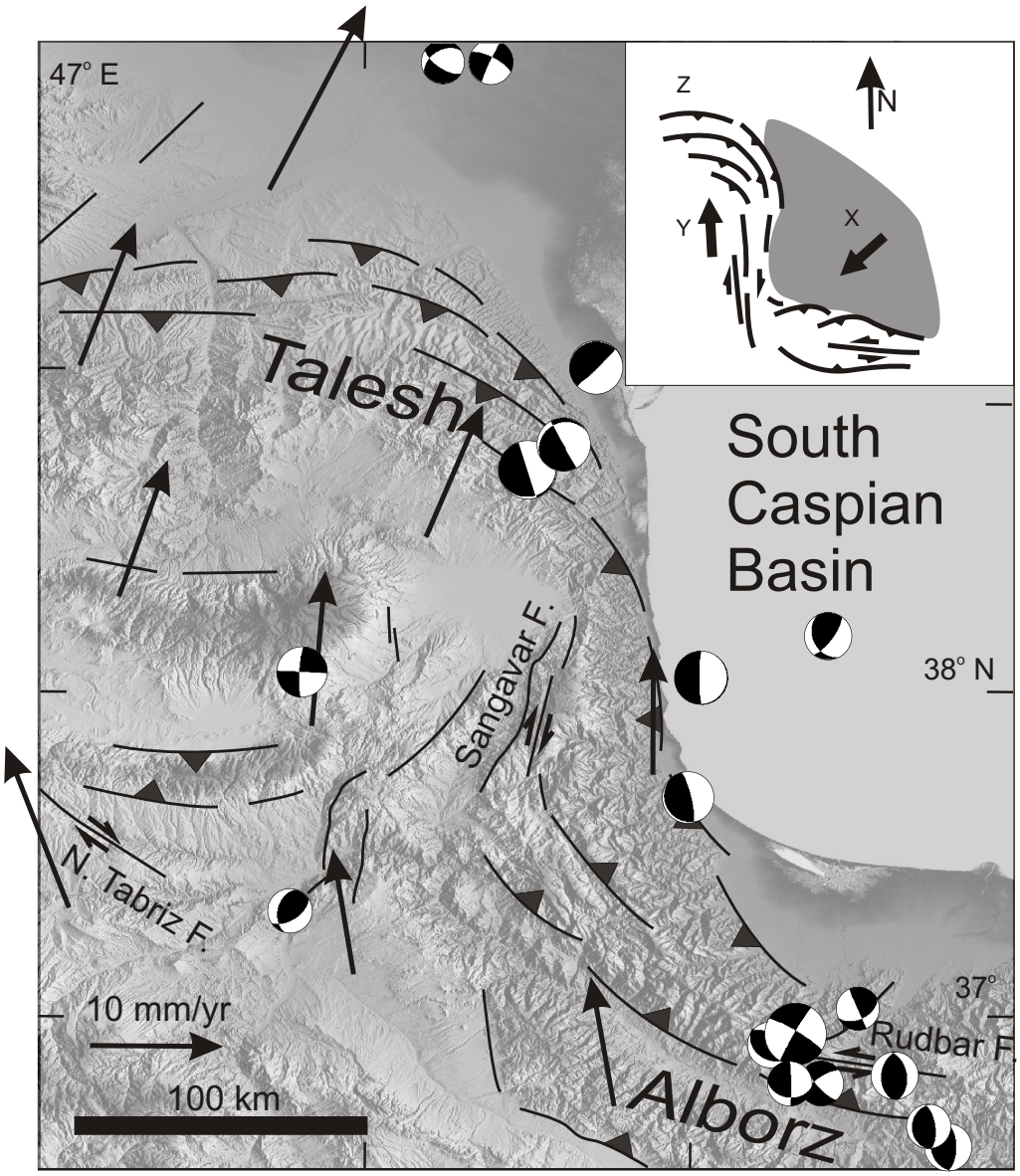
47° E
Z
N
Y
X
Talesh
South
Caspian
Basin
38° N
Sangavar F.
N. Tabriz F.
10 mm/yr
100 km
37°
Rudbar F.
Alborz